

PAPER: ANNALS OF GLACIOLOGY 2002; INTERNATIONAL GLACIOLOGICAL SOCIETY

**SCIENCE GOALS FOR A MARS POLAR CAP SUBSURFACE MISSION:
OPTICAL APPROACHES FOR INVESTIGATIONS OF INCLUSIONS IN ICE**

Frank Carsey, Jet Propulsion Laboratory, California Institute of Technology, Pasadena CA 91104, USA

Email: fcarsey@jpl.nasa.gov

Claus T. Mogensen, Jet Propulsion Laboratory, California Institute of Technology, Pasadena CA 91104, USA and University of Copenhagen, Copenhagen, Denmark.

Alberto Behar, Jet Propulsion Laboratory, California Institute of Technology, Pasadena CA 91104, USA

Hermann Engelhardt, Geophysics, California Institute of Technology, Pasadena CA 91025

Arthur L. Lane, Jet Propulsion Laboratory, California Institute of Technology, Pasadena CA 91104, USA

ABSTRACT. The Mars Polar Caps are highly interesting features of Mars and have received much recent attention with new and exciting data on morphology, basal units, and layered outcroppings. We have examined the climatological, glaciological, and geological issues associated with a subsurface exploration of the Mars North Polar Cap and have determined that a finescale optical examination of ice in a borehole, to examine the stratigraphy, geochemistry and geochronology of the ice, is feasible. This information will enable reconstruction of the development of the cap as well as prediction of the properties of its ice. We present visible imagery taken of dust inclusions in archived Greenland ice cores as well as in-situ images of accreted lithologic inclusions in West Antarctica, and we argue for use of this kind of data in Mars climate reconstruction as has been successful with Greenland and Antarctic ice core analysis.

INTRODUCTION

We have closely examined a potential Mars polar cap mission called Cryoscout; it relies on a cylindrical, tethered subsurface descent vehicle called the Cryobot (Zimmerman et al, 2002; French et al, 2001), a thermal probe that combines the passive heating of the Philberth Probe (Aamot, 1968; Philberth, 1976) with the forced heat transfer of hot-water drilling (Engelhardt et al, 1999) through a heated jet in the nose. It will be powered by a solar photovoltaic system at the surface. In the design and development of the Cryobot, key factors included the low ambient temperature of Mars ice, dust inclusions, overpressure protection, instrument integration, cleanliness, and the initial entry into the ice.

The science data of the mission will be acquired at the surface, with the tether, and on the Cryobot. The surface station will obtain meteorological and visual image data; the tether will be used as the temperature profiler using a commercially available Raman scattering system (Forster et al, 1997); and the Cryobot will be a platform for optical sensors for

system (Forster et al, 1997); and the Cryobot will be a platform for optical sensors for examining the ice, geochemical sensors for the meltwater, and an IR optical absorption instrument for oxygen isotope determination.

In general the ice cap subsurface domain is the archive of the atmospheric processes of the present, with a direct link to the past, including especially the climate and planetary history in the sedimentary record. We note that subsurface ice sites are older, warmer, protected from surface processes, and characterized at Mars temperatures by interstitial liquid water containing concentrated salts. And, the north cap rests on the seafloor of the putative early Mars ocean. The Mars North Polar Cap is topographically quite similar to Greenland although its temperature profile, microstructure and resulting mechanical properties are probably significantly different.

Our science plan is to accomplish the determination of the recent climate history of Mars, the description and analysis of the structure, stratigraphy, and sedimentology of the cap, the characterization of present-day polar surface/atmosphere interactions, and a constraint on the evidence of Mars life through chemical and physical assessment of the meltwater.

MARS AND EARTH ICE

An important consideration is that we have no information about microscopic character of the ice that makes up the Mars North Polar Cap; the appearance of the surface is not a useful indicator of the nature and density of inclusions or horizons. The key to obtaining suitable data on the properties of Mars ice caps is in the design of an exploratory polar cap mission and its instrumentation, of which the optical systems for the visible stratigraphy and dust character are significant. In taking steps to obtain the optical data we begin by noting that the polar cap ice may be clear in the fashion of deep ice sheet ice from Greenland or Antarctica, or it may have sufficient dust and bubbles to be opaque, or somewhere in between. We therefore address the two situations, one in which we can acquire data in light transmission/scattering, and one in which we collect data only in reflection (recognizing a special case of light penetration of millimeters). We have developed techniques for obtaining data for these cases in different sites in Earth's ice sheets, taken to be possible analogs of Mars polar caps, and this paper addresses those techniques.

ICE BOREHOLE CAMERA

The Ice Borehole Camera (IBC) was designed, built and deployed in Ice Stream C by a JPL-Caltech team (Carsey et al, 2002). It utilized downlooking and sidelooking cameras in geometry much like what could be utilized on a Mars Cryobot. It did not deploy a dust sensing system as its objectives primarily addressed accretion ice. The Ice Stream C ice was relatively clear such that macroscopic lithic inclusions could be seen even if a few centimeters beyond the borehole wall. Quantification of these inclusions calls for stereo analysis. Sample IBC images, including stereo pairs, have been discussed (Carsey et al, 2002; Behar et al, 2001), and we show here only one, previously unpublished, series (Figure 1).

The IBC sidelooking image data can be characterized as showing:

- Well-defined layers of accreted basal lithologic material separated by clear ice.
- Regions of the ice sheet with scattered isolated clasts of basal material.
- Clear ice.
- Bubbly ice.
- The roof of a subglacial "lake" about 1.4 m deep.

The IBC downlooking image data can be characterized as showing:

- Uneven hot-water drill melting at the sidewall, probably the consequence of the inclusions.
- Bed material.
- Basal water flow. In figure 1 three frames of downlooking data are shown to illustrate the flow of water at the base of Ice Stream C taken in the 2000-2001 study. The flow is visible in filaments of fine debris being advected toward the top of the image and demonstrating that the basal hydrology is active at this point. Flow is visible because the water has entrained a small amount of bed material, probably loess. If the material is in too great or too small concentration the flow cannot be visualized with this technique, but if the water is too opaque as a result of the hot-water drill suspending it, it will clear in time if the hydrology is in fact active.

JPL LASER DUST NEPHELOMETER

Standard digital camera images are of great value as descriptive data, and these data can be quantitatively interpreted for such variables as the distribution and size of large inclusions. Many other kinds of information are available using optical interrogation, and we demonstrate here that Mie scattering for dust analysis is at least as useful for in-situ observations as for the well-established core analysis (Ram and Koenig, 1997) at finer resolution than with other in-situ strategies (Bay et al, 2000). If the Mars ice is sufficiently clear that extinction lengths of several centimeters are realized, quantitative analysis of included dust can be addressed. We recognize here that Earth ice sheet ice has very little in the way of impurities (~0.01%), and that Mars ice may bear significantly greater dust (perhaps 20%).

Dust in ice sheets has long been known to vary by season and on longer terms due to climate change (Dahl-Jensen et al, 1997; Hammer et al, 1978; Petit et al, 1999; Ram and Koenig, 1997; Steffensen, 1997). For these concentrations optical techniques are well established, first on meltwater and then on bubble-free ice itself, for assessment of dust burden as it varies with depth and consequently time. In the bubble-free part of the core, light was scattered by dust particles, (Ram et al, 1995) over a dynamic range from a few to over 10,000 relative units. Later the GISP2 optics were calibrated (Ram et al, 2000) to cover a range of dust loading to over 10,000 mg/kg, and the signal intensity was linear with dust mass, as required for single-scattering. We note that the results of Steffensen on melt-water and the scattering profiles of Ram et al are not suited to 1:1 comparison for several reasons, but they agree in substance. Light scattering from microbubbles associated with pressure relief long after ice core removal was a problem for deep ice

from cold intervals having high impurities was a problem for Ram et al 2000, and is probably a source of error for this work as well. The crucial facts are that adequate climatically driven dynamic range exists, in the deep ice of Greenland, with particles suited to assessment by optical scattering as predicted for the single-scattering regime.

Dust in the ice can be said to come from three sources: ordinary atmospheric transport, dust storms, and volcanic eruptions. Both GRIP and GISP2 dust analyses find the particle size distributions close to power-law in form with means in radius near 1 micron for both background dust and dust storms and for all climate conditions. A detailed and thorough analysis of the dust storm events and the background dust in the GISP2 ice (Donarummo, 1997) shows that the size distribution is modified to somewhat larger particles and the total dust mass is increased dramatically (in excess of an order of magnitude) during dust storms compared to background transport. The GRIP ice dust was comprehensively analyzed by Steffensen (1997) with results similar to GISP2 including a small shift of size distribution peak upward with colder climates, from about 0.9 micron (Holocene) to 1 micron (LGM). Total dust mass ranged from less than 50 mg/kg (recent) to over 7000 mg/kg (LGM), and again the total dust mass is distributed strongly (84-99%) in the particle range centered at 1 micron radius. Petit et al (1999) examined ice from East Antarctica and their results also show particles clustered near 1 micron radius with slight increase in size for glacial periods.

Particles near 1 micron radius constitute an ideal size distribution for optical measurement. Mars atmospheric dust has been optically examined and found to be in the same size range (Tomasko et al, 1999; Ockert-Bell et al, 1997), as would be expected given that the deposition rate for this dust is pressure independent. Clearly the Mars ice caps are expected to contain dust, and the dust should be in the size range for optical investigation using visible wavelength light. The only real issue is that of total dust mass loading; if Mars ice has too much dust mass (or too little, an unlikely possibility) the Mie assumptions will not supply interpretable signal strength.

In figure 2 we show the predicted detected power (Baron and Willeke, 2001), per 1000 particles, for light scattering from the Greenland distribution of dust particles (Steffensen, 1997). Of interest is the flattening of the curve near 120° and the relative insensitivity to wavelength. To utilize this scattered power, the observational geometry of Figure 3 is employed. Note that the scattering angle varies from about 90° where the laser beam enters the camera field of observation on the right and increases to about 130° where the beam exits. This geometrical set up is accomplished with an ice core using equipment as configured in Figure 4. This geometry was used at the National Ice Core Laboratory (NICL) using an SBIG astronomical camera and solid state red laser, and data were taken using a variety of exposure times and angles.

An image of data taken from 2503 m in the GISP2 core is shown in Figure 5 where the laser beam crosses the image from right to left near the center of the frame; layers of dust can clearly be seen in this negative image. Two aspects of the scattering are worthy of note. First note that the less-dusty levels are remarkably clear and well defined; also, note that the dusty intervals are characterized by measured light from above and below

(in the figure) center of the beam. This light is almost certainly due to multiple scattering. The image data are shown in Figure 6 in a 3-dimensional format. The sharp peaks are taken to be light scattering from bubbles and other large inclusions, possibly present as a result of the 9 years that this ice has been resting at one atmosphere pressure. In Figure 7 a single row from an image is displayed along with a Gaussian fit to the curve with maximum near row 400 as this represents the path of the laser beam; each camera pixel represents 40 microns of ice. Note that the Gaussian is a reasonable approximation to the curve. When the Gaussian smoothing is applied to the whole image, the 3-dimensional representation in Figure 8 is the result. Strictly speaking the peaks of the curves should be strongly analogous to the laser light scattering results of Ram et al (1997).

In figure 9 we show 3 cm of images with the laser dust nephelometer system compared to the Ram et al results (as acquired from the National Snow and Ice Data Center). To construct Figure 9 images were acquired on 5 mm translations of the camera-laser down the core, and the separate image data are shown as different lines. Note that the image to image correlation is very good. In the lower graph of Figure 9 the Ram et al data are shown; these data are archived at 1 mm resolution at 2500 m depth. It is not possible at this time to locate precisely the laser nephelometer data with respect to the archived laser scattering data as depth could not be determined accurately due to an uneven core end, but the similarity in spatial data strongly suggests that the same dust signal is being investigated, as it should be since the basic measurement principle is the same, only the geometry is slightly different.

CONCLUSIONS

We have discussed and demonstrated methods of acquisition of simple but scientifically useful image data from Mars ice cap ice involving a range of ice clarity from opaque ice to clear ice with banded dust inclusions analogous with Earth ice sheet ice. The nature of Mars ice cap ice is completely unknown and open to speculation for now. The general approach of optical examination can be taken considerably further of course, most notably through the use of analytical fluorescence and Raman scattering methods, which are well developed for laboratory work. It is our intention to develop these additional means of interrogating ice with optical methods for future investigations of ice of Earth, Mars and Europa.

ACKNOWLEDGEMENTS

We acknowledge the excellent collaboration with Prof. Barclay Kamb in the Ice Borehole Camera project and the contribution of NSF-OPP in supporting field work in Ice Stream C. We got excellent support from the National Ice Core Laboratory and the National Snow and Ice Data Center. We also acknowledge the work done in the definition of the Cryoscout mission by the Science and Engineering Teams including F. S. Anderson, N. Bridges, S. Clifford, P. Conrad, D. Fisher, M. Hecht, J. Head, K. Herkenhof, J. Johnson, S. Kounaves, R. S. Saunders, R. Warwick and W. Zimmerman. This work was

performed ^{at} by the Jet Propulsion Laboratory, ~~a division of~~ ^g California Institute of Technology, under contract to NASA.

REFERENCES

- Aamot, H., *Instrumented Probes For Deep Glacial Investigations*, USACRREL Technical Report 210, 1968.
- Bay, R., P. Price, G. Clow, and A. Gow, Climate logging with a new rapid optical technique at Siple Dome, *Geophys. Res. Lett.*, 2001.
- Baron, P. and K. Willeke, *Aerosol Measurement: Principles, Techniques, and Applications*, Wiley-Interscience, 1131 p, 2001.
- Behar, A., F. Carsey, A. Lane, and H. Engelhardt, the Antarctic ice borehole probe, Proc. IEEE Aerospace Conference, Big Sky, MO, March, 2001. Track 2, #2.0511
- Carsey, F., H. Engelhardt, A. Lane, a. Behar, A Borehole Camera System For Imaging The Deep Interior Of Ice Sheets, *Journ. Glac.*, in press, 2002.
- Dahl-Jensen, D., T. Thorsteinsson, R. Alley and H. Shoji, Flow properties of the ice from the Greenland ice Core Project ice core: the reason for folds?, *Journ. Geophys. Res.*, 102, 26831-26840, 1997.
- Donarummo, John Jr, *Analysis of high dust concentration events in pre-Holocene ice from the Summit core*, MA Thesis, State University of New York, 1997.
- Engelhardt, H., B. Kamb, and R. Bolsey, A hot-water ice-coring drill, *J. Glaciology*, 1999.
- Forster, A., J. Schrotter, D. Merriam, and D. Blackwell, Application of optical-fiber temperature logging--an example in a sedimentary environment, *Geophysics* 62, 1107-1113, 1997.
- French, L., F. Anderson, F. Carsey, G. French, A. Lane, P. Shakkottai, W. Zimmerman, and H. Engelhardt, Cryobots: An answer to subsurface mobility in planetary icy environments, Proc ISAIRAS Montreal, 2001.
- Hammer, C., H. Clausen, W. Dansgaard, N. Gunderstrup, W. Johnson and N. Reeh, Dating of Greenland ice cores by flow models, isotopes, volcanic debris and continental dust, *J. Glac.* 20, 3-26, 1978.
- Ockert-Bell, M., J. Bell III, J. Pollack , C. McKay and F. Forget, Absorption and scattering properties of the Martian dust in the solar wavelengths, *Journ., geophys. Res.*, 102, 9039-9050, 1997.

- Petit, J.-R., et al, Climate and atmospheric history of the past 420,000 years from the Vostok ice core, Antarctica, *Nature*, 429-436, 1999.
- Philberth, K., The thermal probe deep-drilling method by EGIG in 1968 at Station Jarl-Joset, Central Greenland, 19-22, in: Splettstoesser, J. F., *Ice-Core Drilling*, University of Nebraska Press, 1976.
- Ram, M., M. Illing, P. Weber, G. Koenig, and M. Kaplan, Polar ice stratigraphy from laser-light scattering: Scattering from ice, *Geophys. Res. Lett.*, 24, 3525-3527, 1995.
- Ram, M. and G. Koenig, Continuous dust concentration profile of pre-Holocene ice from the Greenland ice Sheet Project 2 ice core: Dust stadials, interstadials, and the Eemian, *Journ. Geophys. Res.*, 102, 26642-26648, 1997.
- Ram, M., J. Donarummo jr., M. Stolz, and G Koenig, Calibration of laser-light measurements of dust concentration for Wisconsinan GISP2 ice using instrumental neutron activation analysis of aluminum: Results and discussion, *Journ. Geophys Res.*, 105, 24731-24738, 2000.
- Steffensen, J. The size distribution of microparticles from selected segments of the Greenland Ice Core Project ice core representing different climatic periods, *J. Geophys. Res.*, 102, 1273-1285, 1997.
- Tomasko, M., L. Doose, M. Lemmon, P. Smith and E. Wegryn, Properties of dust in the Martian atmosphere from the imager on Mars Pathfinder, *Journ. Geophys. Res.*, 104, 8987-9007, 1999.
- Zimmerman, W., F. Anderson, F. Carsey, P. Conrad, H. Engelhardt, L. French, and M. Hecht, The Mars '07 north polar cap deep penetration Cryoscout mission, IEEE Aerospace Conference, Big Sky, Montana, Session 2.07, Missions, Systems and Instruments for In Situ Exploration, March 9-16.

Figure Captions

Figure 1. Downlooking images from the Ice Borehole Camera deployed at 1225 m in Ice Stream C, Antarctica. A chain, as an aid to determining depth of viewing, and a compass, out of focus in this picture, are visible as is the borehole wall. This kind of image is designed to provide data on bed nature and relative movement.

Figure 2. Predicted scattering using Mie equations for a collection of particles with the size distribution of Steffensen (1997). The use of particles in a range of sizes tends to wash out the lobes present in single-size calculations.

Figure 3. A cartoon of an ice core with dusty layers with oblique laser illumination and a camera to record scattered light.

Figure 4. As in Fig. 3 except a CAD drawing of the observational system for using oblique laser scattering with an ice core. The core has a flat on one side as is usual for modern cores.

Figure 5. A negative image taken in the geometry of Fig. 4. Here the laser light is across the image from right to left, and the dark band across the center represents light scattered by dust. Other black spots are due to bubbles in the ice; they are large and very efficient scatterers of even stray light. Note the abruptness of the dusty to clear transition.

Figure 6. A three dimensional representation of the scattering image shown in Fig. 5. Note that the noise peaks off the laser track (and possibly those on the laser track as well) are narrow and can be very tall (bright).

Figure 7. One row from a scattering image. Here the dust data is represented by the maximum around 400 pixels and bubble scatter noise can be seen near 200 and 500 pixels. The smooth line is a Gaussian fit to the data near pixel 400.

Figure 8. As in Fig. 6 a three dimensional representation of the scattering image, but this time the "data" shown are the Gaussian best-fits as demonstrated in fig. 7.

Figure 9. Top: Gaussian area vs depth acquired by the Laser Nephelometer. The different lines are from different frames of data, with the camera and laser translated 5 mm for for each frame. Bottom: Laser Light Scattering (LLS) data from GISP2 (Ram et al) acquired from NSIDC. We have taken the liberty of moving along the Ram et al data a few centimeters to obtain an optimal fit as the core end is quite uneven, and it was not possible to tell precise depth.

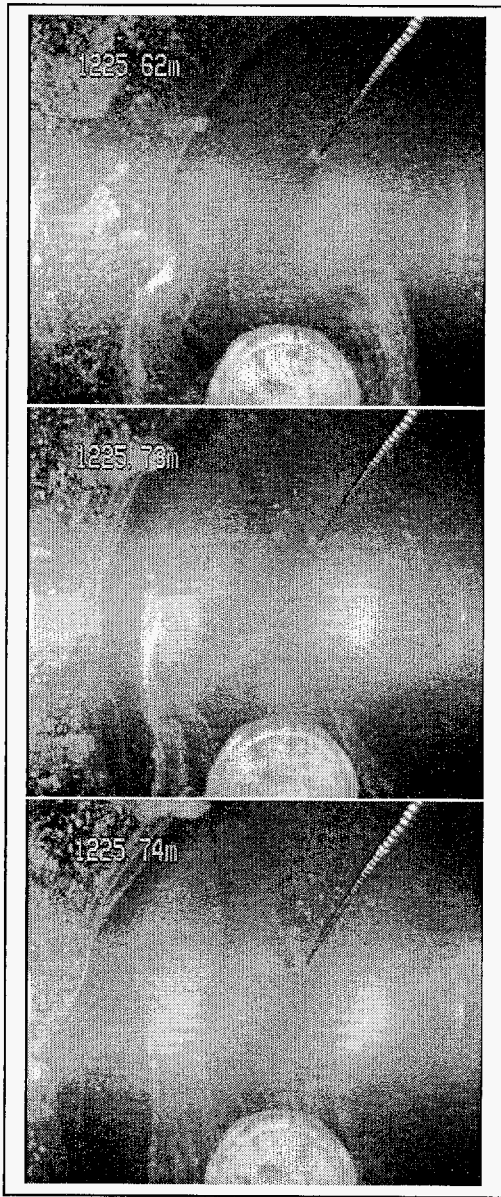


Figure 1

Figures

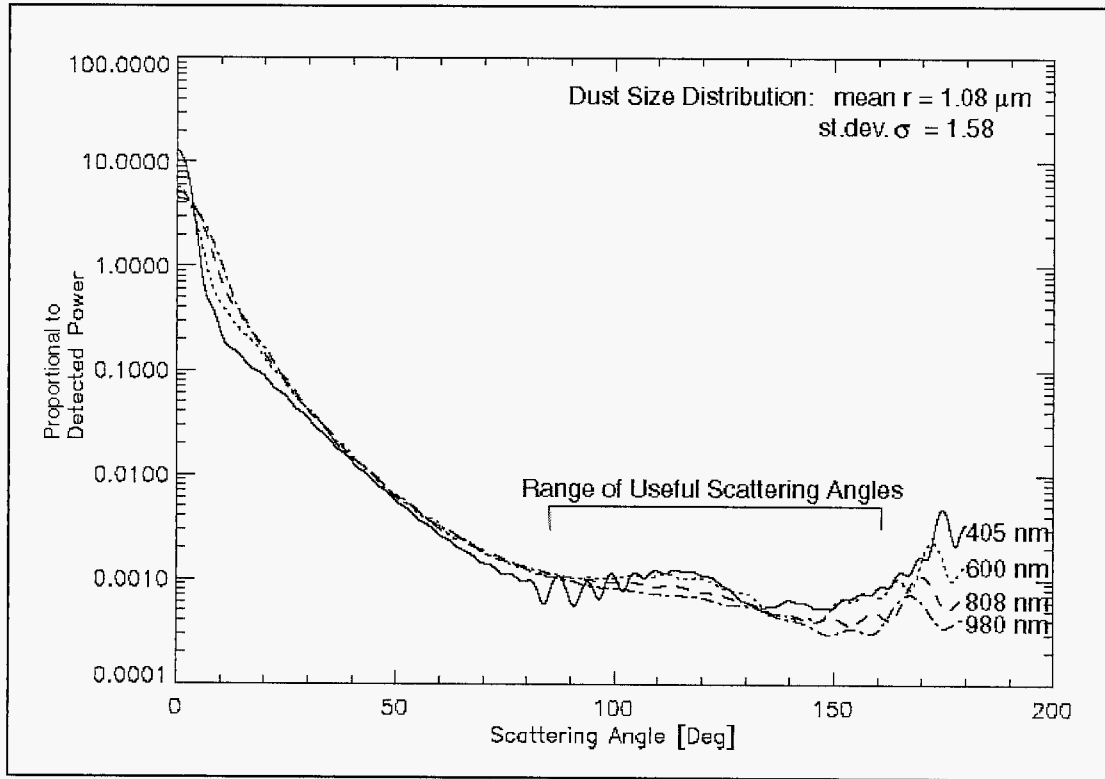


Figure 2

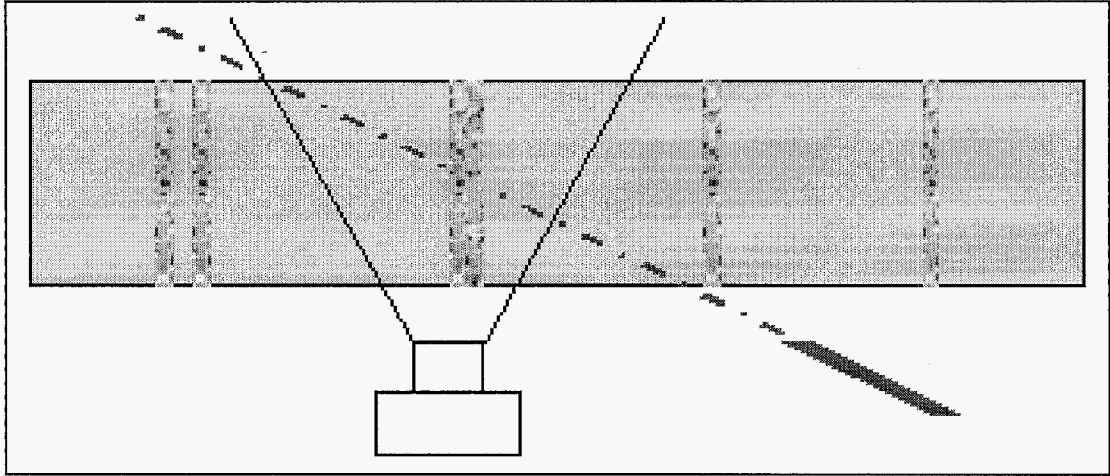


Figure 3

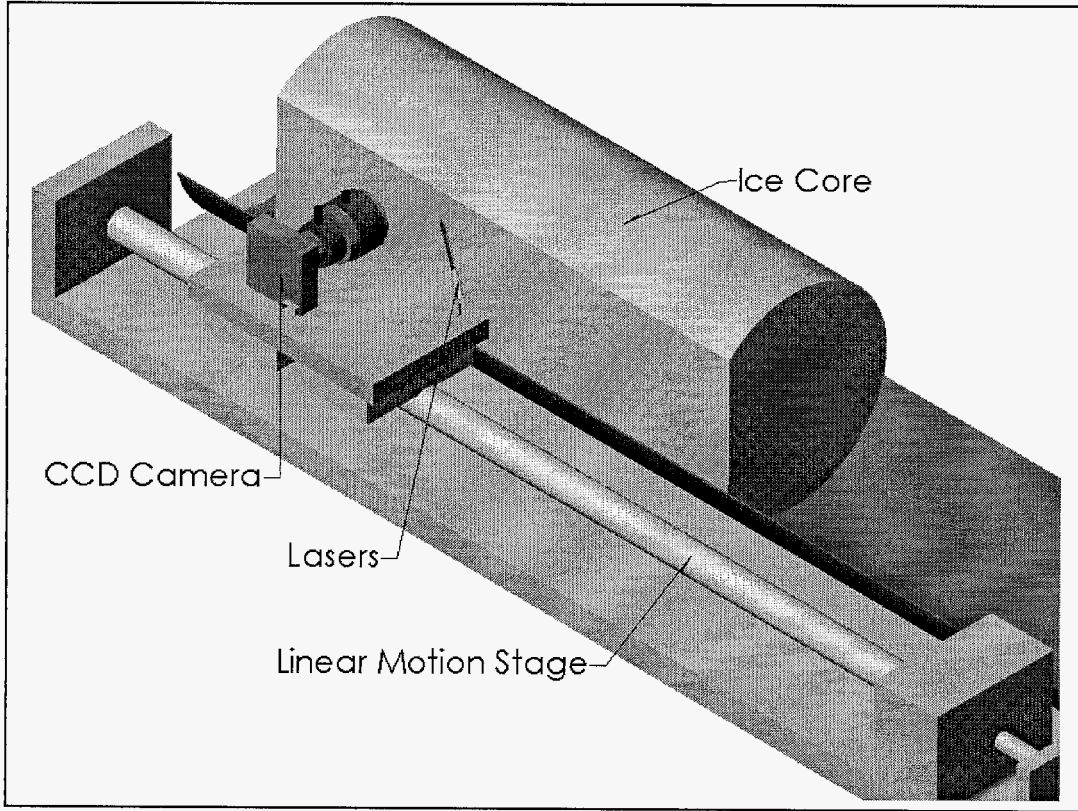


Figure 4

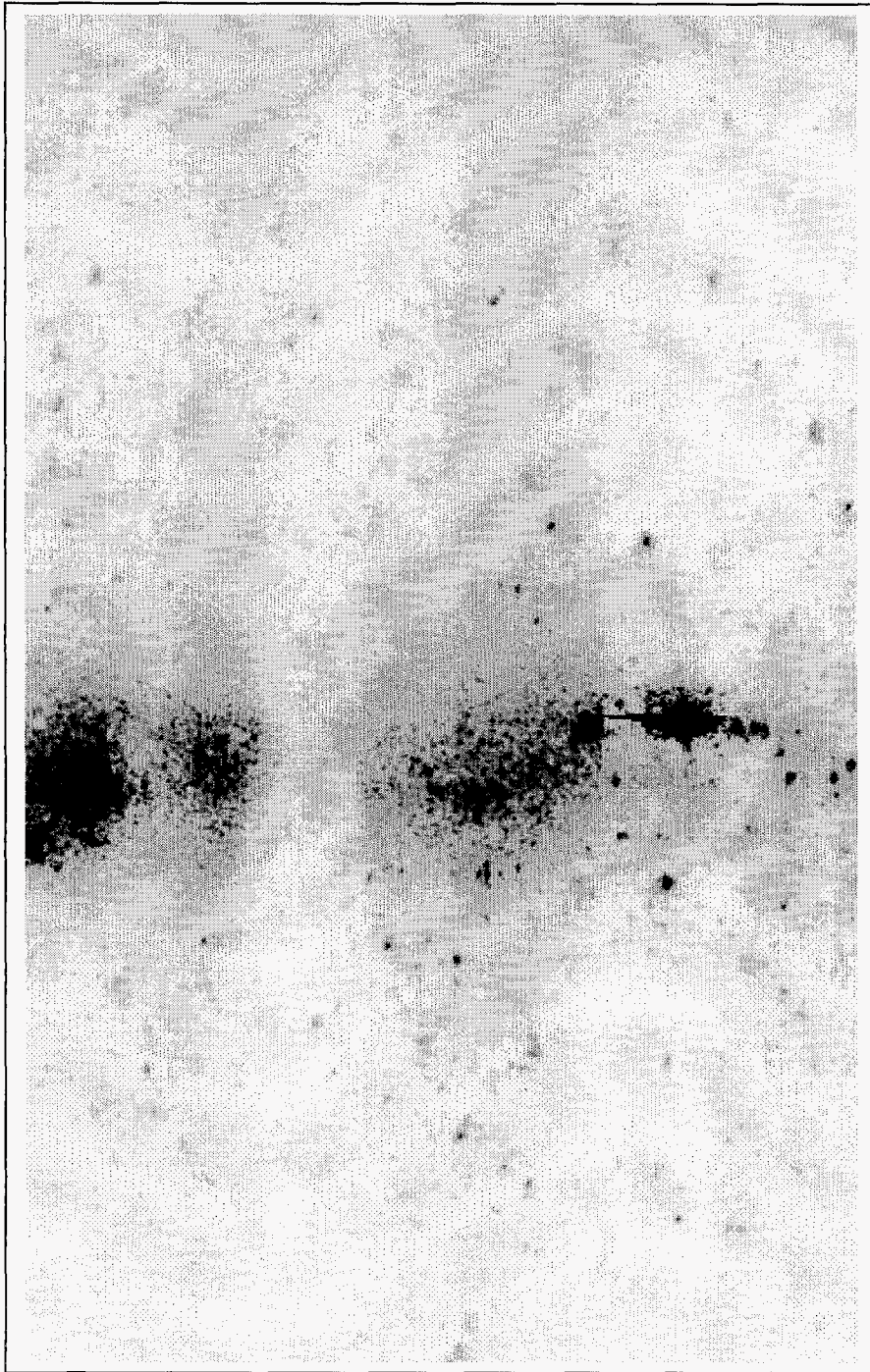


Figure 5

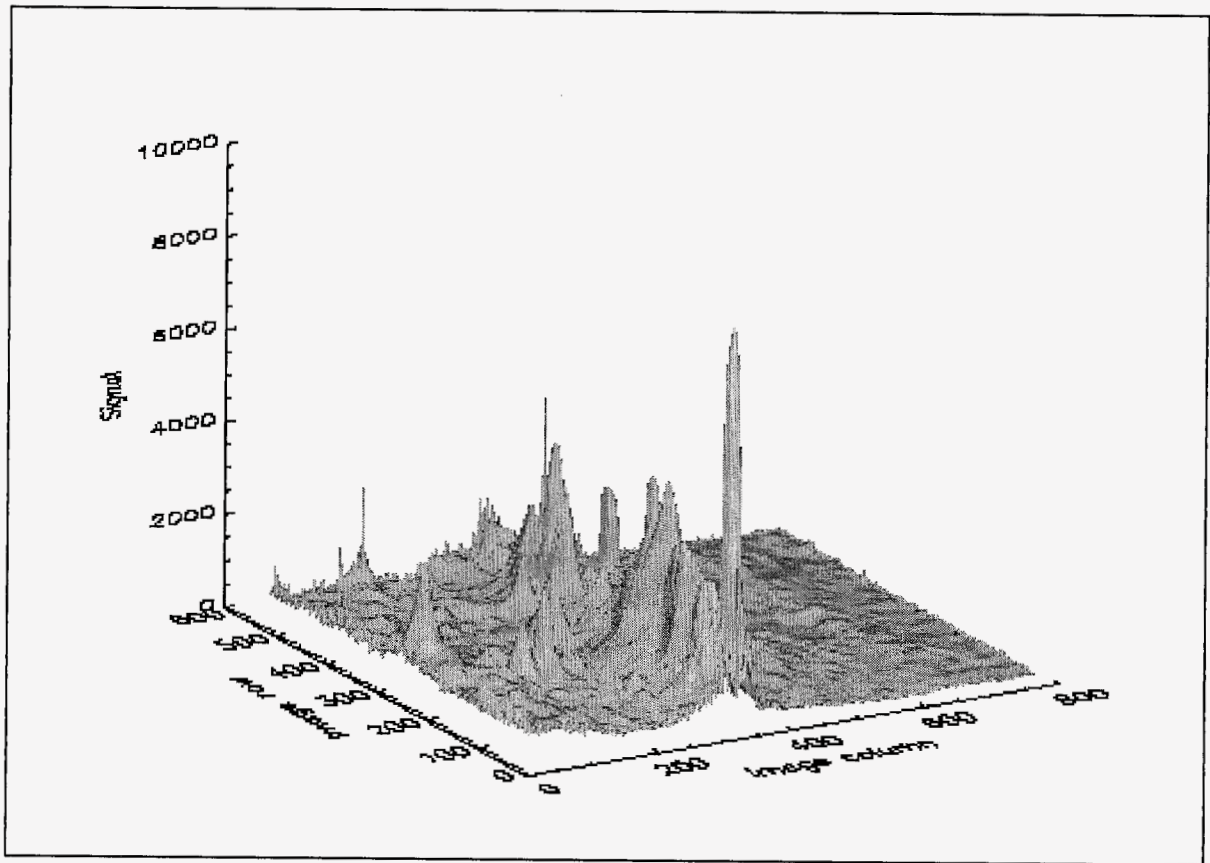


Figure 6

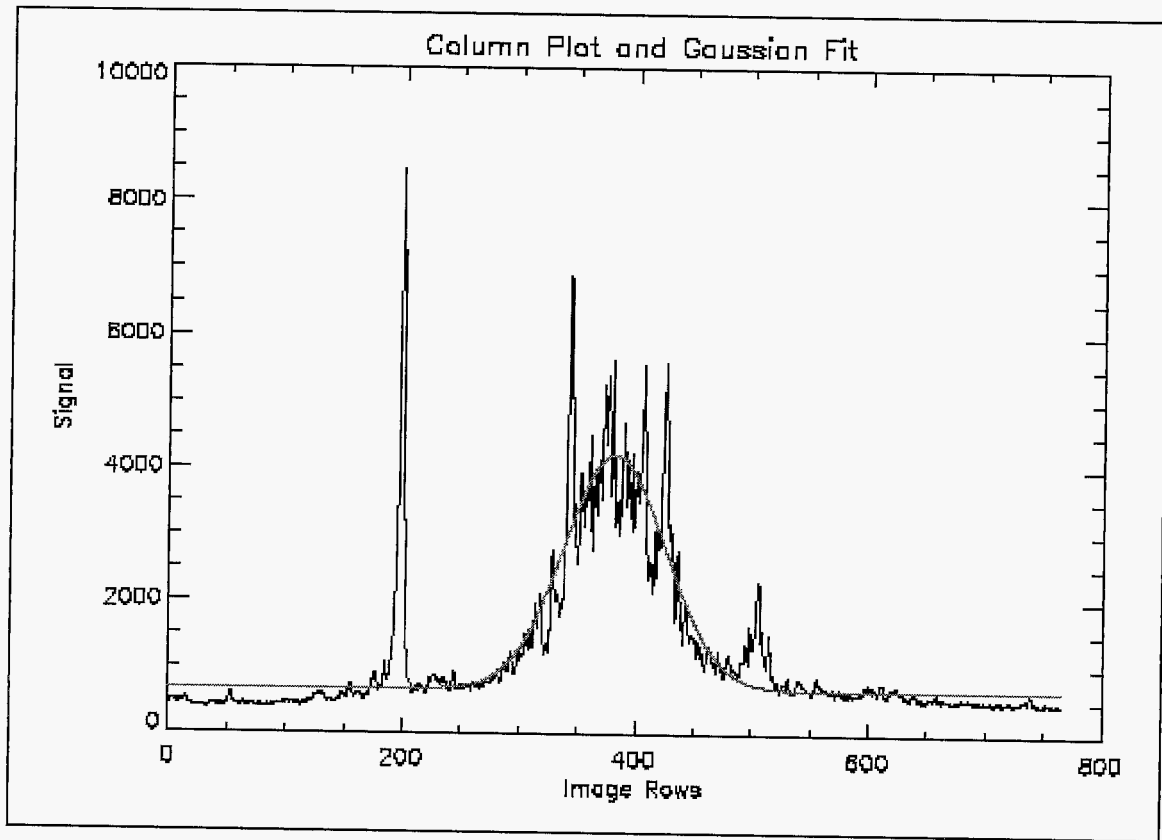


Figure 7

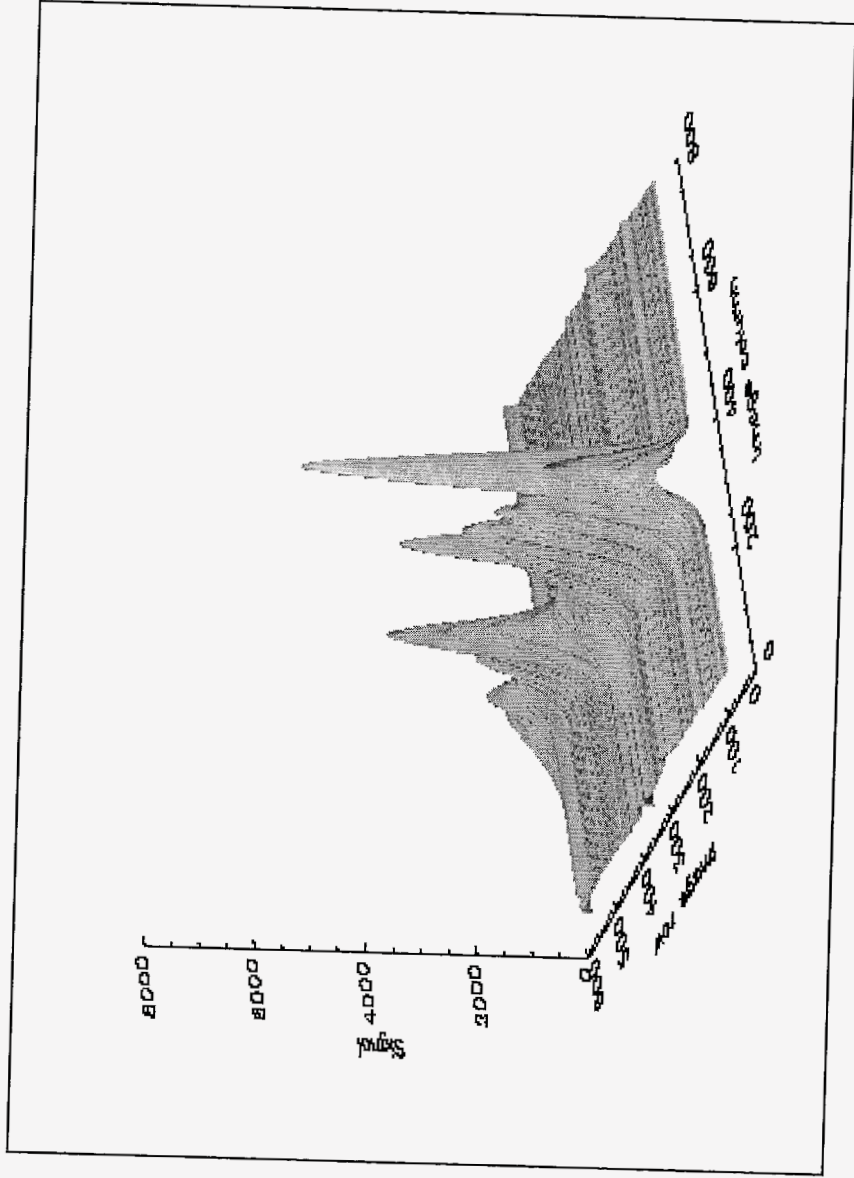


Figure 8

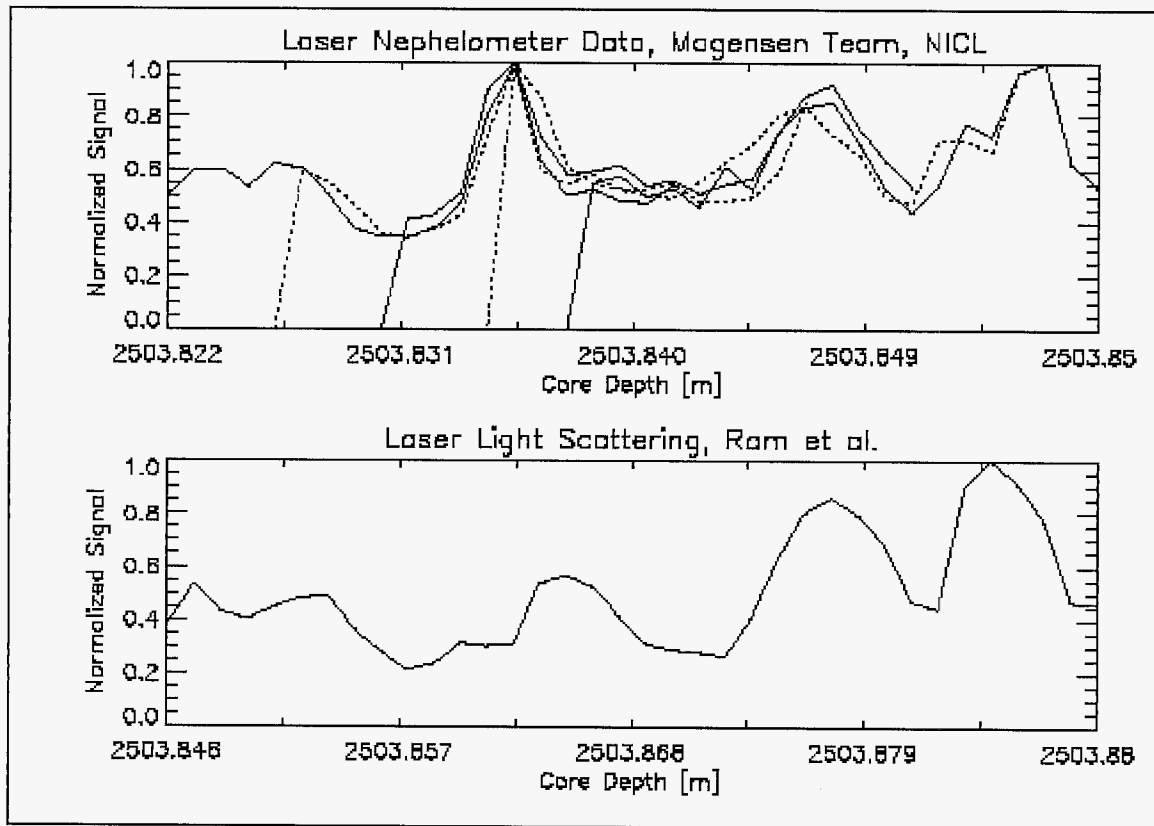


Figure 9

End of File

